Diradical character and second hyperpolarizability of multidecker inverse sandwich complexes of Mg and Ca

ARTICLE *in* CHEMICAL PHYSICS LETTERS · APRIL 2015

Impact Factor: 1.9 · DOI: 10.1016/j.cplett.2015.03.055

2 AUTHORS:

Kaushik Hatua

Indian Institute of Engineering Science and …

13 PUBLICATIONS **48** CITATIONS

SEE PROFILE

Prasanta Nandi

Indian Institute of Engineering Science and …

17 PUBLICATIONS **102** CITATIONS

SEE PROFILE

Chemical Physics Letters 628 (2015) 1–8

Contents lists available at ScienceDirect

Chemical Physics Letters

journal homepage: www.elsevier.com/locate/cplett

Diradical character and second hyperpolarizability of multidecker inverse sandwich complexes of Mg and Ca

Kaushik Hatua, Prasanta K. Nandi*

Department of Chemistry, Indian Institute of Engineering Science and Technology, Shibpur, Howrah 711103, India

ARTICLE INFO

Article history:
Received 13 October 2014
In final form 30 March 2015
Available online 6 April 2015

ABSTRACT

The ground state structures of first- and second-order inverse sandwich (**MIS-I** and **MIS-II**) complexes (M-(C_4H_4-M)$_n$, n = 1 and 2) of Mg and Ca have been found to be singlet diradical while the third-order complexes **MIS-III** (n = 3) are pure triplet. The second hyperpolarizability of the open-shell singlet complexes **MIS-I** and **MIS-II** are predicted larger than the analogs triplets. The magnitude of second hyperpolarizability enhances on replacing Mg with Ca metal atom. The larger second hyperpolarizability of **MIS-I** compared to that of **MIS-II** of the same metal may be attributed to the intermediate singlet diradical character of the former.

1. Introduction

In search of potential NLO active materials to meet the increasing demand in photonic devices, optical data storage, data processing and data transmission, a large number of theoretical and experimental efforts have been spent for the past few decades [1–6]. Apart from inorganic crystals ($LiNbO_3$, KH_2PO_4) organometallic compounds having interesting NLO characteristics draw special attention in this field. The notable design of potential third order NLO active materials includes hexalithiobenzene (10^6 a.u.) [7], long chain polyyne and polyene (10^6–10^7 a.u.) [8–12], radical ion-pair salt (10^6 a.u.) [13], open shell intermediate diradical species (10^6 a.u.) [14–17], metal incorporated organic framework (10^6 a.u.) [18], halofullerenes (10^6 a.u.) [19,20], lithiated silicone cage (10^6 a.u.) [21], etc. Incorporating light metal atoms in suitable hydrocarbon part may result in strong enhancement of hyperpolarizabilities. Recently, we have considered a number of beryllium (Be) based organometallic systems [22–25] which showed large second hyperpolarizability (γ). The strong enhancement of γ in these complexes has been ascribed to the stronger ground state polarization and facile electronic coupling with the low lying excited states. It has been noted [25] that the double coned inverse sandwich complex (Be–C_4H_4–Be) possesses about 40 times larger amplitude of the longitudinal component of γ (at the CAM-B3LYP/6-311++G(d,p) level) compared to the normal sandwich (C_4H_4–Be–C_4H_4) complex. Inspired with this result, we continued to add Be–C_4H_4 decking unit over Be–C_4H_4–Be to form multidecker inverse sandwich (MIS) complexes of order 'n' having general formula Be-(C_4H_4-Be)$_n$ ($n \neq 0$). The complex Be–C_4H_4–Be is known as MIS of first order and labeled as **MIS-I**. The component of second hyperpolarizability along the molecular axis increases with increasing size of **MIS** complexes. With an anticipation that the more electropositive metal can offer the more polarized ground state, the lighter beryllium metal has been replaced by the larger members of alkaline earth metals, i.e. magnesium and calcium metal atoms. In the present work, a number of model **MIS** complexes of Mg and Ca up to third order M-(C_4H_4-M)$_n$ (n = 1–3) has been considered for a comparative theoretical study of their structure and second hyperpolarizability. Among the investigated metal complexes, the structure of Ca–C_4H_4–Ca has been considered in the recent theoretical study of Ca–Ca interaction in Ca–C_8H_8–Ca complex by Liu et al. [26] who obtained open-shell singlet as the ground state. The optimized structures of the chosen **MIS** complexes are shown in Scheme 1.

2. Computational methods

Geometry optimization of the multidecker inverse sandwich complexes in open-shell singlet and triplet has been carried out by using the spin-unrestricted B3LYP (UB3LYP) [27] method and 6-311++G(d,p) basis set. The closed shell structures are obtained by using the RB3LYP/6-311++G(d,p) method. The $\langle S^2 \rangle$ values of the open-shell singlet complexes calculated using the symmetry-broken method at the UB3LYP/6-311++G(d,p) level with the option IOP (5/14 = 2) have been found to vary within 0.87–0.99. The frequency calculations showed that the optimized geometries

* Corresponding author.
E-mail address: nandi_pk@yahoo.co.in (P.K. Nandi).

http://dx.doi.org/10.1016/j.cplett.2015.03.055
0009-2614/

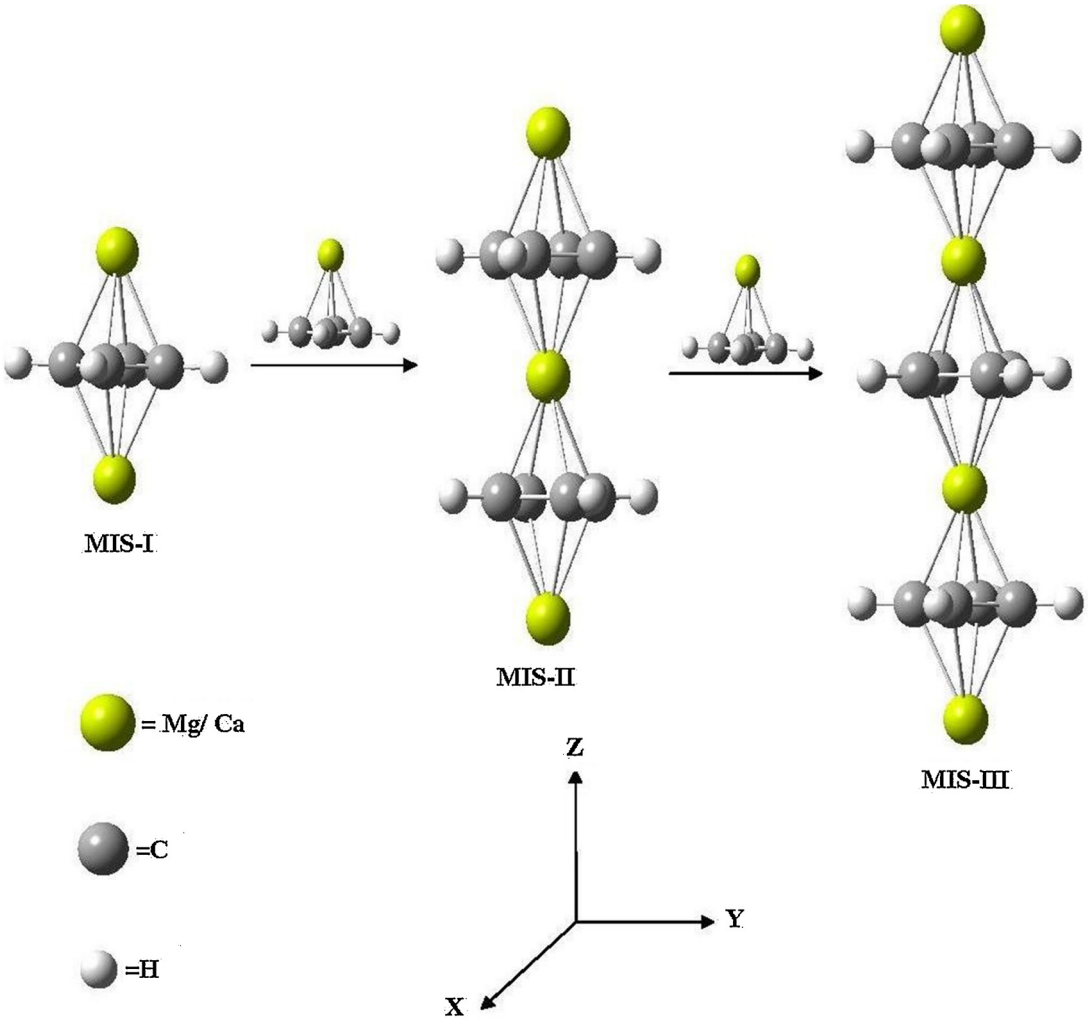

Scheme 1. The UB3LYP/6-311++G(d,p) optimized structures of multidecker inverse sandwich complexes of magnesium and calcium.

(Scheme 1) have no imaginary vibrational frequencies. Natural population analysis (NPA) has been carried out to examine the extent of ground state polarization of the investigated metal complexes.

The singlet diradical character of the investigated metal complexes has been calculated by using two approaches. In the first case, the diradical index (y_{PUHF}) related to HOMO and LUMO orbitals is defined by the weight of the doubly-excited configuration in the MC-SCF theory and is formally expressed in the spin projected UHF (PUHF) theory [28,29] as

$$y_{(PUHF)} = 1 - \frac{2T}{1+T^2} \tag{1}$$

where T is the overlap between the corresponding orbital pairs that can also be expressed in terms of the occupation numbers (n) of UHF natural orbitals.

$$T = \frac{n_{HOMO} - n_{LUMO}}{2} \tag{2}$$

In the present PUHF calculation of diradical character, the symmetry-broken UB3LYP/6-311++G(d,p) optimized geometry has been used. The diradical character (y_{PUHF}) 0% and 100% corresponds to the closed-shell and pure diradical states, respectively. In the second approach the diradical index (y_{CASSCF}) has been calculated from the occupation number of the LUMO obtained from the CASSCF (2,4) calculation performed at the RB3LYP/6-311++G(d,p) optimized geometry.

When an external electric field interacts with a molecule, an induced dipole moment is created due to the deformation of electronic charge distribution. The electric dipole moment can be expressed by the following Taylor series expansion in the static field of magnitude F_0,

$$\mu = \mu_0 + \alpha F_0 + \frac{1}{2!}\beta F_0^2 + \frac{1}{3!}\gamma F_0^3 \ldots\ldots\ldots \tag{3}$$

where μ_0 is the permanent dipole moment and the coefficients α, β, and γ are called polarizability, first hyperpolarizability and second hyperpolarizability of the molecule, respectively. The Cartesian components of dipole second hyperpolarizability are evaluated by numerical differentiation of the analytically obtained first hyperpolarizability by using the spin-unrestricted DFT (UDFT) method consisting of BHHLYP [30], long range corrected CAM-B3LYP [31] and LC-BLYP [32] functional. The spin projected UHF, UMP2 and UCASSCF methods are also used to compare with the UDFT calculated results. The electric field strength has been varied within 0.00001–0.0001 a.u. to check the numerical stability of the calculated dipole second hyperpolarizability of the investigated metal complexes. In our previous study [22,25], we have noted that the 6-311++G(d,p) basis set is adequate for reproducing comparable results of second hyperpolarizability obtained at much larger basis sets like aug-cc-pVXZ (X = D and T). Furthermore the use of double augmented basis set d-aug-cc-pVDZ obtained by adding another set of diffuse functions does not enhance the second

Table 1
B3LYP/6-311++G(d,p) calculated energy differences (kcal/mol) between the closed-shell singlet and the open-shell symmetry-broken singlet ($\Delta E_{CS\text{-}OS}$)[a], singlet-triplet energy gap ($\Delta E_{T\text{-}OS}$)[b] along with the diradical character y (%) and orbital overlap (T) obtained by using the PUHF and CASSCF(2,4) approaches.

Metal	Complex	$\Delta E_{CS\text{-}OS}$	$\Delta E_{T\text{-}OS}$	$y_{(PUHF)}$	T	$y_{(CASSCF)}$
Mg	MIS-I	8.112	2.696	57	0.224	76
	MIS-II	19.588	0.050	94	0.028	97
	MIS-III	23.188	−0.012	100	0.000	100
Ca	MIS-I	0.336	0.332	80	0.099	89
	MIS-II	14.680	0.023	98	0.009	99
	MIS-III	0.005	−16.227	100	0.000	100

[a] Energy of closed-shell singlet-energy of open-shell singlet.
[b] Energy of triplet-energy of open-shell singlet.

hyperpolarizability to an appreciable extent [25]. Thus the chosen 6-311++G(d,p) basis set is expected to give reliable results of second hyperpolarizability. All calculations have been performed by using the G09 program [33].

3. Results and discussion

3.1. Optimized structure and diradical character

The energy differences between the closed-shell singlet and open-shell singlet, open shell triplet and singlet obtained at the B3LYP/6-311++G(d,p) level, and the PUHF and CASSCF(2,4) calculated percentage diradical character obtained for the chosen molecular complexes are reported in Table 1. The two sets of y values show an identical trend. The singlet diradical character obtained for the **MIS-I** complex of Ca is fairly consistent with the recent theoretically calculated results obtained by Liu et al. [26]. As can be seen **MIS-I** and **MIS-II** complexes represent intermediate diradical systems while the third-order complexes are pure diradical systems. The ground states of third order complexes of both metals are found to be triplet diradical. The high spin complex Ca **MIS-III** lies about 16.23 kcal/mol lower in energy than the closed shell singlet or open shell singlet states. For M-(C_4H_4-M) and M-(C_4H_4-M)$_2$ (M = Mg and Ca) complexes the ground state is the open shell singlet. The CASSCF(6,6) calculations shows the multiconfiguration nature of the singlet state of **MIS-I** and **MIS-II** complexes as follows. For Mg complexes: $^1\psi_{\mathbf{MIS\text{-}I}}$ = 0.61 [222000] + 0.35 [220200]; $^1\psi_{\mathbf{MIS\text{-}II}}$ = 0.19 [222000] + 0.16 [220200] + 0.64 [221100]. For Ca complexes: $^1\psi_{\mathbf{MIS\text{-}I}}$ = 0.55 [222000] + 0.42 [220200]; $^1\psi_{\mathbf{MIS\text{-}II}}$ = 0.49 [222000] + 0.48 [220200] + 0.02 [221100]. The T_1 diagnostic approach of Lee [34] considered for the lowest order MIS complex of Mg and Ca yield a value of 0.02 at the CCSD level.

The important optimized geometrical parameters and natural atomic charges (q) are given in Table 2 for open shell singlet and triplet diradicals since for these spin states the energy differences are relatively smaller except for the **MIS-III** complex of Ca (see Table 1). For the later complex the energy difference between the closed-shell and open-shell singlets is negligibly small. The larger $r_{CC\text{-}M}$ distance in MIS compounds of Ca compared to that of Mg compounds is due to the larger atomic size of calcium. The distance between the terminal metal and cyclobutadiene ring ($r_{CC\text{-}M}$) decreases by about 0.01 Å in both Mg and Ca complexes on increase of the size of complex. This substantially longer metal-ring distance in **MIS-I** complexes may arise from the migration of spin-up and spin-down electrons toward the opposite direction of M—M bonding under the influence of C_4H_4 ring (due to formation of stable aromatic sextet, $C_4H_4^{2-}$) to produce singlet diradicals ($\dot{M}-(C_4H_4)-\dot{M}$). The tendency of separating electron pair having opposite spins will be energetically favored if they are subsequently be involved in bonding with other M-C_4H_4 units so that radical pair are generated on metal atoms at a longer distance strongly favoring the parallel spin state as in the **MIS-III** complex ($\dot{M}-(C_4H_4)-\{M-(C_4H_4)-M\}-(C_4H_4)-\dot{M}$). The spin flipping (singlet diradical → triplet diradical) leads to triplet ground state of **MIS-III** (Table 1). However, the variation of the average distance between the central metal atom and C_4H_4 ring is different in the low and high spin metal complexes. In Mg complexes, $r_{CC\text{-}M}$ shortens by 0.017 Å (in **MIS-II**) and 0.029 Å (in **MIS-III**) with respect to the corresponding terminal metal-ring distances while in the Ca complex, the corresponding distances increase by about 0.03 Å (in **MIS-II**) and 0.02 Å (in **MIS-III**). This sort of differential variation of $r_{CC\text{-}M}$ distances in Mg and Ca complexes may be due to the greater ionic character of bonding with calcium metal. It should be noted that in singlet diradicals, the average distance ($r_{CC\text{-}CC}$) between two successive rings containing Ca atom (4.638 Å in **MIS-II**/4.704 Å in **MIS-III**) is appreciably larger than that containing Mg atom (4.046 Å/4.035 Å) which is due to the larger size of calcium atom. The comparable $r_{CC\text{-}CC}$ distances in open-shell *singlet* and *triplet* **MIS-II/MIS-III** complexes (Table 2) arises from the

Table 2
Calculated distance between the end metal atoms (r_{MM}, Å), shortest M-C_4H_4 distance ($r_{CC\text{-}M}$, Å), average distance between two successive C_4H_4 rings ($r_{CC\text{-}CC}$, Å), and natural atomic charges on metal (q_M, a.u.) atom of open-shell singlet and triplet diradical metal complexes obtained at the UB3LYP/6-311++G(d,p) level.

	Multidecker inverse sandwiches of Mg			Multidecker inverse sandwiches of Ca		
	MIS-I	MIS-II	MIS-III	MIS-I	MIS-II	MIS-III
Singlet diradical						
r_{MM}	4.102	8.127	12.151	4.658	9.343	14.051
$r_{CC\text{-}M}$	2.049	2.040[a], 2.023[b]	2.040[a]2.011[b]	2.329	2.319[a]2.353[b]	2.321[a]2.345[b]
$r_{CC\text{-}CC}$		4.046	4.035		4.638	4.704
q_M	0.741	0.740[a] 1.375[b]	0.736[a]1.370[b]	0.798	0.782[a]1.481[b]	0.784[a]1.472[b]
Triplet diradical						
r_{MM}	4.105	8.127	12.150	4.656	9.353	14.053
$r_{CC\text{-}M}$	2.051	2.041[a] 2.023[b]	2.040[a]2.011[b]	2.328	2.323[a]2.354[b]	2.321[a]2.346[b]
$r_{CC\text{-}CC}$		4.045	4.035		4.707	4.705
q_M	0.748	0.740[a] 1.376[b]	0.736[a]1.370[b]	0.797	0.740[a]1.376[b]	0.784[a]1.472[b]

[a] End C_4H_4 or M atom.
[b] Central C_4H_4 or M atom.

Table 3
Longitudinal component of second hyperpolarizability (γ_{zzzz}, 10^6 a.u.) of multidecker inverse sandwich compounds of Mg and Ca obtained for open shell singlet and triplet states by different methods.

	Singlet diradical		Triplet		
	MIS-I	MIS-II	MIS-I	MIS-II	MIS-III
γ_{zzzz} of Mg MIS complexes					
UHF	0.507	0.638	0.465	0.621	0.772
UBHHLYP	1.944	1.453	0.584	0.911	1.206
UCAM-B3LYP	1.717	1.222	0.545	0.837	1.103
LC-UBLYP (μ = 0.47)	0.6990.921	0.6310.794	0.3980.452	0.5590.670	0.6990.855
LC-UBLYP (μ = 0.33)					
UMP2	1.1702.561	0.5730.988	0.815	0.594	2.524
UCASSCF					
γ_{zzzz} of Ca MIS complexes					
UHF	2.004	2.484	1.951	2.459	2.807
UBHHLYP	4.802	2.950	2.004	2.566	2.940
UCAM-B3LYP	3.333	2.551	1.839	2.346	2.686
LC-UBLYP (μ = 0.47)	1.3271.293	1.9832.069	1.5531.597	1.9382.020	2.1942.282
LC-UBLYP (μ = 0.33)					
UMP2	2.7912.291	1.9441.098	1.954	1.907	1.055
UCASSCF					

The γ_{zzzz} values obtained for **MIS-I/MIS-II** complexes are calculated at the UCASSCF(6,6)/UCASSCF(2,2) level.

negligible effect of unpaired electron spins on the terminal metals on the metal-ring bonds within the chain. This result is again consistent with the ease of spin flipping in higher-order **MIS** complexes. The magnitude of charge on central metal atoms is almost twice of that of the end metal atoms which is fairly consistent with the presence of unpaired electrons residing on terminal metal atoms corresponding to the open-shell singlet and triplet structures of metal complexes. The greater extent of charge transfer from calcium arises from its larger size.

3.2. Dissociation energy

In the following are given the different scheme of dissociation of the chosen inverse sandwich metal complexes. The energy calculation has been carried out by considering the ground state of **MIS-I** and **MIS-II** as open shell singlet and the ground state of **MIS-III** state as triplet. The complete dissociation into neutral and ionic fragments are considered. The former mode of dissociation involves relative much lower energy. The D_{2h} structure of cyclobutadiene molecule being the lower energy isomer compared to the other isomer having C_{2V} symmetry has been used in the calculation of energy of dissociation into neutral species.

MIS-I	**Energy (kcal/mol)**
M-(C_4H_4-M) = M-C_4H_4 + M	*E* = 41.83/51.76 (Mg/Ca)
M-C_4H_4 = M^{+2} + $C_4H_4^{2-}$	*E* = 623.15/551.57 (Mg/Ca)
M-(C_4H_4-M) = M + M^{+2} + $C_4H_4^{2-}$	*E* = 664.98/603.33 (Mg/Ca)
M-(C_4H_4-M) = 2 M + C_4H_4 (D_{2h})	*E* = 17.06/68.50 (Mg/Ca)
MIS-II	
M-(C_4H_4-M)$_2$ = M-(C_4H_4-M) + M-C_4H_4	*E* = 71.13/70.89 (Mg/Ca)
M-(C_4H_4-M) = M-C_4H_4 + M	*E* = 41.83/51.76 (Mg/Ca)
2M-C_4H_4 = 2M^{+2} + 2$C_4H_4^{2-}$	*E* = 1264.30/1103.14 (Mg/Ca)
M-(C_4H_4-M)$_2$ = M + 2M^{+2} + 2$C_4H_4^{2-}$	*E* = 1377.26/1225.79 (Mg/Ca)
M-(C_4H_4-M)$_2$ = 3M + 2C_4H_4 (D_{2h})	*E* = 60.08/159.94 (Mg/Ca)
MIS-III	
M-(C_4H_4-M)$_3$ = M-(C_4H_4-M)$_2$ + M-C_4H_4	*E* = 72.31/70.90 (Mg/Ca)
M-(C_4H_4-M)$_2$ = M-(C_4H_4-M) + M-C_4H_4	*E* = 71.13/70.89 (Mg/Ca)
M-(C_4H_4-M) = M-C_4H_4 + M	*E* = 41.83/51.76 (Mg/Ca)
3M-C_4H_4 = 3M^{+2} + 3$C_4H_4^{2-}$	*E* = 1869.45/1654.71 (Mg/Ca)
M-(C_4H_4-M)$_3$ = M + 3M^{+2} + 3$C_4H_4^{2-}$	*E* = 2054.72/1848.26 (Mg/Ca)
M-(C_4H_4-M)$_3$ = 4M + 3C_4H_4 (D_{2h})	*E* = 112.14/225.23 (Mg/Ca)

An interesting point of difference may be noted between the two schemes of dissociation. The ionic dissociation of Ca complexes involves relatively smaller energy compared to that of Mg complexes. The difference of dissociation energy increases with increasing size of complexes. This result indicates that Ca metal owing to its larger size should favor ionic interaction. However, in the case of dissociation into neutral fragments, Ca complexes need higher energy compared to Mg complexes. Again the difference increases with increasing size of complexes. The metal–ligand interaction energy can be estimated as the average energy of the steps leading to the overall ionic dissociation and follows the order **MIS-I** (332.5/301.7) < **MIS-II** (459.1/408.6) < **MIS-III** (513.7/462.1) for Mg/Ca complexes. The larger/smaller metal–ligand interaction energy associated with Mg/Ca metal accounts for the significant decrease of $r_{CC\text{-}Mg}$/increase of $r_{CC\text{-}Ca}$ distances of the metal—C_4H_4 bond in the central region of **MIS-II/III** complexes (Table 2). The chosen complexes are significantly stable toward dissociation into free metal and ligand and the stability increases with increasing size of the complex and metal atom which is reflected in the variation of calculated dissociation energy: **MIS-I** (17.1/68.5) < **MIS-II** (60.1/159.9) < **MIS-III** (112.1/225.2). The energy required to expel a metal atom from an MIS complex calculated as the average of energies associated with the reactions involved varies in the order: **MIS-I** (41.8/51.8) < **MIS-II** (56.5/61.3) < **MIS-III** (61.8/64.5).

3.3. Static electronic second hyperpolarizability

Owing to the molecular alignment the charge transfer takes place along the *z* axis (see Scheme 1). The results of the longitudinal component of static second hyperpolarizability (γ_{zzzz}) obtained for the open-shell diradical singlet (**MIS-I/II**) and triplet (**MIS-I/II/III**) complexes of Mg and Ca calculated by using the spin-unrestricted methods (PUHF, UDFT, PUMP2 and UCASSCF) are reported in Table 3. The UHF calculated values obtained for Mg complexes are significantly smaller compared to that of Ca complexes. However, at this level invariably lager γ_{zzzz} has been predicted for **MIS-II** compared to **MIS-I** for both Mg and Ca. At the correlated levels (UBHHLYP, UCAM-B3LYP, UMP2 and UCASSCF) γ_{zzzz} of **MIS-I** complexes is predicted larger than that of **MIS-II** complexes of same metal although the order of magnitudes does not changed. The CCSD calculated result of γ_{zzzz} (3.164×10^6 a.u.) obtained for the **MIS-I** of **Ca** is fairly consistent with the UCAM-B3LYP result: 3.333×10^6 a.u. The CCSD γ_{zzzz} (2.969×10^6 a.u.) of **MIS-I** of Mg is, however, significantly larger than that predicted at the UBHHLYP UCAM-B3LYP level but comparable to the UCASSCF(6,6) result: 2.561×10^6 a.u.

The performance of LC-BLYP functional has been examined by considering the range separating parameter (μ) as 0.47 and 0.33, respectively. For the singlet diradical Mg complexes γ_{zzzz} enhances by about 31.8% (in **MIS-I**) and 25.8% (in **MIS-II**) while for the triplet

complexes it enhances by 13.6%, 19.9% and 22.3% in **MIS-I**, **MIS-II** and **MIS-III**, respectively at lower value of μ. The use of different range separating parameter, however, changes the γ_{zzzz} value of Ca complexes by about 3–4%. This DFT method, however, fails to predict the correct qualitative trend of γ_{zzzz} for singlet **MIS-I** and **MIS-II** complexes of Ca. Among the chosen DFT functionals, the LC-UBLYP method substantially underestimates the magnitude of γ_{zzzz} of the chosen metal complexes. The substantial lowering of γ_{zzzz} of **MIS-II** compared to **MIS-I**, in general, is consistent with the fact that on gradual elongation of H—H bond distance the second hyperpolarizability of the H_2 molecule gradually increases, attains a maximum and then decreases further. The maximum value of second hyperpolarizability of H_2 is obtained at the intermediate diradical region [35]. Since the singlet diradical character (y_{PUHF}) of **MIS-II** (0.94 (Mg)/0.98 (Ca)) is much larger than the **MIS-I** complex (0.57 (Mg)/0.80 (Ca)), γ_{zzzz} of **MIS-II** complex locating radicals on terminal metal atoms lying at a longer distance is predicted smaller (by about 25.2%/58.3% with Mg/Ca at the UBHHLYP level of calculation) than that of **MIS-I** complex. Compared to the high spin **MIS-I** and **MIS-II** complexes, γ_{zzzz} of singlet diradical **MIS-I** and **MIS-II** complexes enhances by an order of magnitude for Mg complexes. The corresponding increase in the case of Ca complexes is relatively small. The magnitude of γ_{zzzz} of high spin metal complexes (triplet) obtained by UHF and UDFT methods increases gradually on increasing size of the complex, **MIS-I** < **MIS-II** < **MIS-III**. The largest magnitude of γ_{zzzz} is obtained for the triplet **MIS-III** complex of calcium.

The relative performance of different DFT methods on the calculated results of γ_{zzzz} obtained for Mg and Ca complexes has been examined in Figures 1 and 2, respectively. The UBHHLYP and UCAM-B3LYP results exhibit an almost identical pattern of

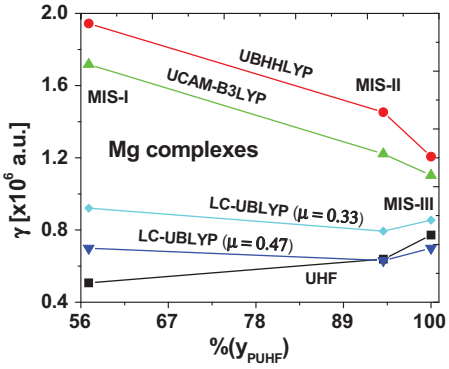

Figure 1. The variation of γ_{zzzz} of Mg complexes with diradical index (PUHF).

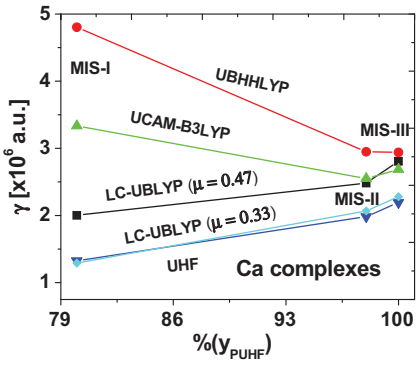

Figure 2. The variation of γ_{zzzz} of Ca complexes with diradical index (PUHF).

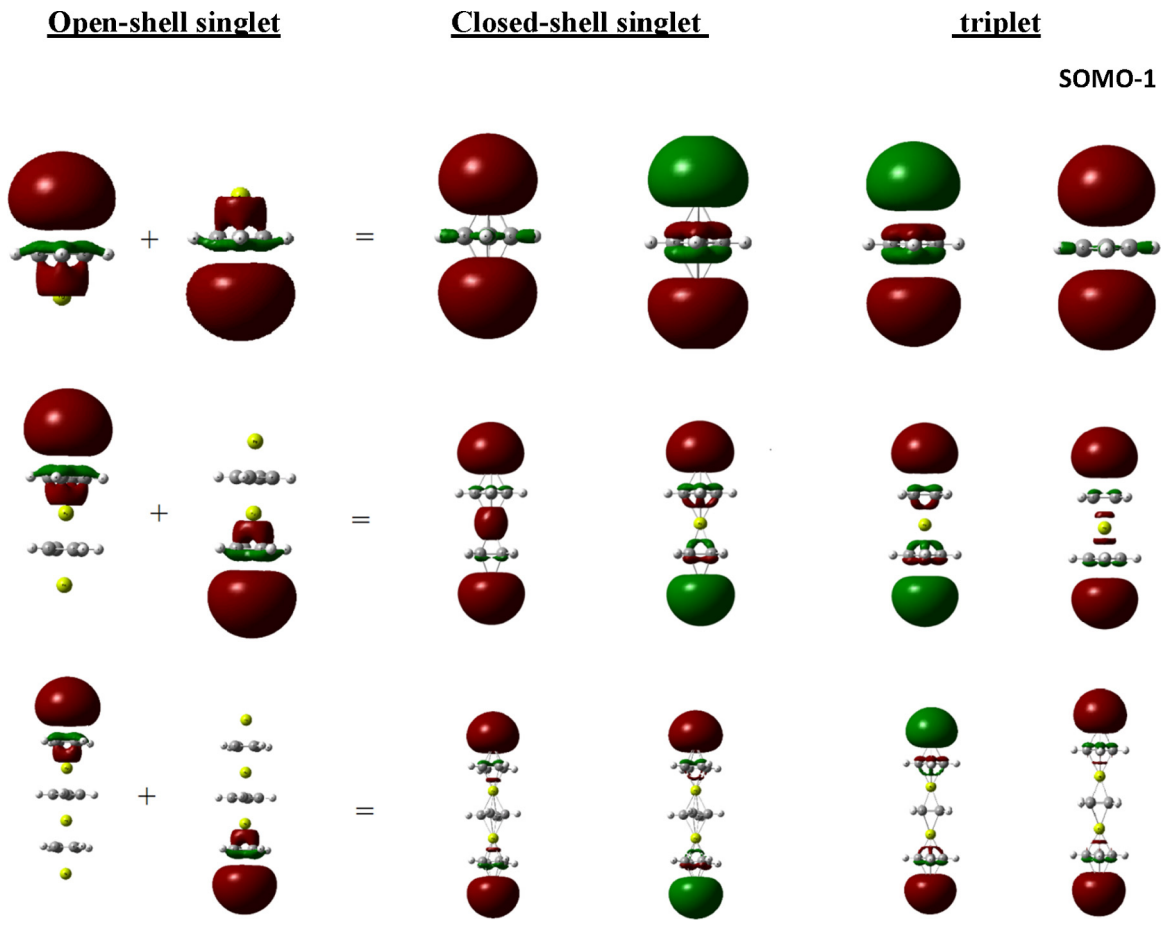

Figure 3. Frontier orbital pictures of open shell singlet, closed shell singlet and open shell triplet wave function of magnesium MIS compounds.

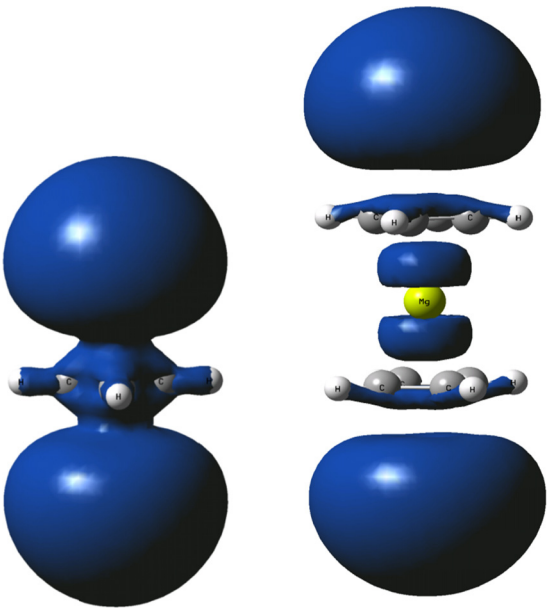

Figure 4. Spin density distribution in open shell triplets of **MIS-I** and **MIS-II** of Mg.

variation i.e. γ_{zzzz} decreases steadily for Mg complexes while for Ca it decreases on passing from **MIS-I** to **MIS-II** complex and then subsequently show a small increase corresponding to the high spin complex **MIS-III**. The UHF and LC-UBLYP calculated results of γ_{zzzz} obtained for Ca complexes vary in the order **MIS-I** (*singlet*) < **MIS-II** (*singlet*) < **MIS-III** (*triplet*). The use of smaller μ in LC-UBLYP enhances the magnitude of γ_{zzzz} of Mg complexes.

The calculated highest occupied α-MO (α-HOMO) and β-MO (β-HOMO) of open-shell singlet, HOMO and LUMO of closed-shell singlet and two singly occupied MOs, SOMO and SOMO-1 of triplet states of Mg complexes are depicted in Figure 3. The spatial diradical distribution in the singlet diradical structures has been examined by inspecting the HOMOs for α and β spin electrons. In Mg-(C_4H_4-Mg) the distribution of α and β spin orbitals clearly show a common region of space (Figure 3) across the cyclobutadiene ring which is consistent with the significant orbital overlap T (Table 1) of the complex. It has been noted that α-HOMO and β-LUMO occupy the same part of space involving about 0.61 and 0.39 electrons. Likewise, the β-HOMO and α-LUMO occupy the same region of space consisting of the other electron. In this way there remain no unpaired electrons in **MIS-I** of Mg although two of them occupy different parts of space. This kind of delocalization of electron pair in the spin orbitals of **MIS-I** complex of Mg accounts for its larger second hyperpolarizability. In **MIS-II** and **MIS-III** complexes of Mg the lobes of α and β spin orbitals reside on two M-C_4H_4 units at the terminal sites. Since the spin orbitals of **MIS-II** and **MIS-III** complexes do not share any common region of space their diradical character is predicted reasonably larger (smaller T) which is close to that of pure triplets and thus lowers the magnitude of γ_{zzzz} (Table 3). It can be seen that the HOMO and LUMO of a closed-shell singlet structure have almost identical shapes as those of SOMO-1 and SOMO of the corresponding triplet structure delocalized mainly over the terminal metal atoms. However, the SOMO extends partly on the C_4H_4

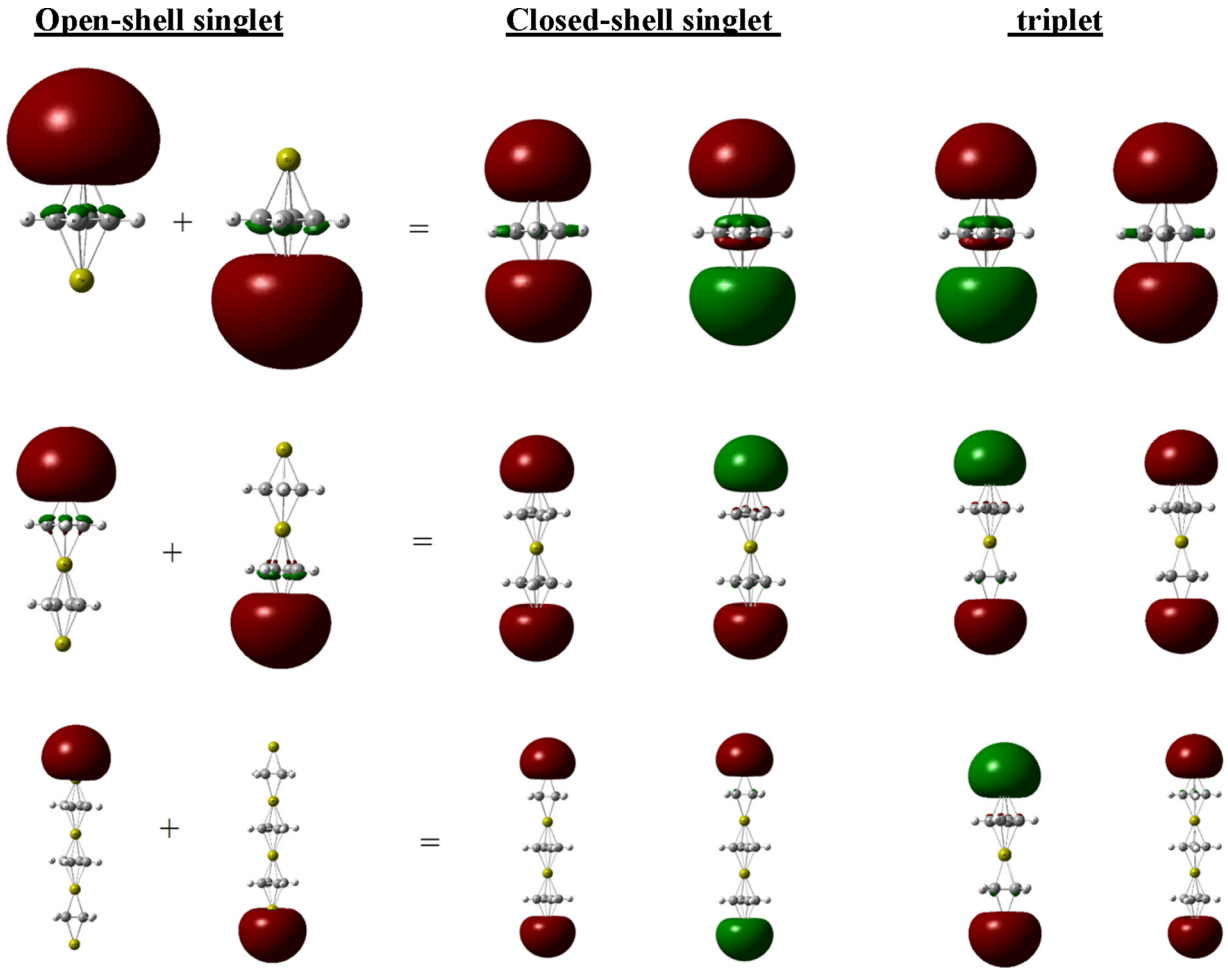

Figure 5. Frontier orbital pictures of open shell singlet, closed shell singlet and open shell triplet wave function of calcium MIS compounds.

Table 4
The spectroscopic properties associated with the most dominant transition calculated by using the **MRCI** method for **MIS-I** and **MIS-II** complexes, and **TD-UCAM-B3LYP** method for the **MIS-III** complex for the 6-311 + +G(d,p) basis set.

	Mg complexes					Ca complexes			
	ΔE_{gn} (eV)	μ_{gn}	f_{gn}	Excitation channel		ΔE_{gn} (eV)	μ_{gn}	f_{gn}	Excitation channel
MIS-I	3.570	5.274	0.38	$S_0 - S_1$	**MIS-I**	2.937	3.420	0.13	$S_0 - S_3$
MIS-II	4.915	3.846	0.28	$S_0 - S_4$	**MIS-II**	3.199	2.706	0.09	$S_0 - S_4$
MIS-III	4.156	2.651	0.67	$S_0 - S_{21}$	**MIS-III**	2.136	2.590	0.35	$S_0 - S_7$

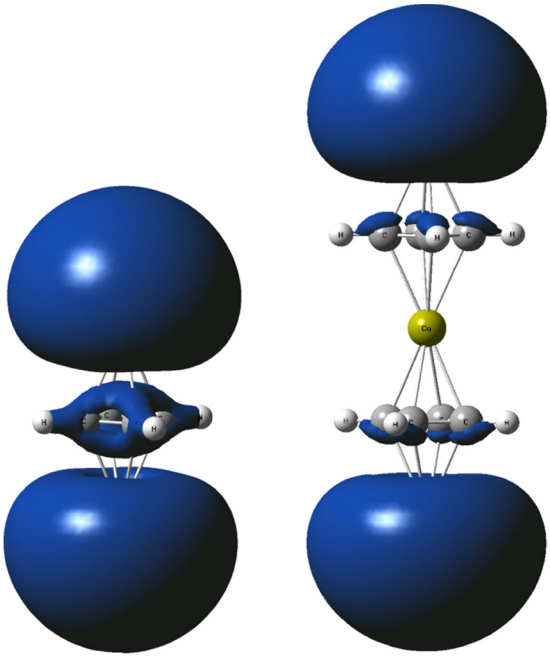

Figure 6. Spin density distribution in open shell triplets of **MIS-I** and **MIS-II** of Ca.

rings adjacent to the terminal metal atoms the extent of which is significant in **MIS-I** and is negligible in **MIS-III** of Mg. This indicates that triplet diradical character of Mg complex increases on going from **MIS-I** to **MIS-III** (with zero overlap of spin orbitals). This is also consistent with the spin density distribution pattern (Figure 4) in the triplet **MIS-I** and **MIS-II** complexes of Mg which clearly shows a sharp decrease of overlap of spin density on increasing size of the complex.

The shapes of the frontier orbitals (Figure 5) obtained for Ca complexes are very much similar to that of Mg complexes (Figure 3). However, some notable point of differences may be noted. As for example, the α-HOMO and β-HOMO of **MIS-I** although do no share any common space like that of Mg complex the corresponding α-LUMO and β-LUMO, however, share a small region of space which is consistent of the rather small value of *T*. Also a small extent of delocalization of LUMO (for closed-shell structure) and SOMO (for triplet structure) over the C_4H_4 ring can be noted only for **MIS-I**. For larger complexes the SOMO and SOMO-1 orbital lobes are concentrated over the terminal Ca atoms which indicate triplet diradical character in the higher order MIS complexes. This has been supported by the spin density distribution in the triplet **MIS-I** and **MIS-II** complexes of Ca (Figure 6).

The electronic transition energy (ΔE_{gn}), transition moment (μ_{gn}) and oscillator strength (f_{gn}) associated with the most dominant transition obtained for the chosen complexes (Table 4) calculated using the multi reference configuration interaction (MRCI) method for **MIS-I** and **MIS-II** (having multiconfigurational nature of the singlet ground state) and TD-UCAMB3LYP method for pure triplet **MIS-III** are used to qualitatively rationalize the variation of cubic polarizability. The general trend of third-order polarizability, **MIS-I** (*singlet*) > **MIS-II** (*singlet*) (Table 3) is fairly consistent with the significant increase of ΔE_{gn} and decrease of μ_{gn}. Although the level of calculations is quite different, the electronic transition in the high spin **MIS-III** is more intense compared to singlet complexes. The relatively smaller second-hyperpolarizability of **MIS-III** (*triplet*) compared to that of **MIS-I** (*singlet*) may arise from the substantial lowering of the transition moment.

4. Conclusions

The investigated multidecker inverse sandwich complexes M-$(C_4H_4$-M$)_n$ (n = 1 and 2) of magnesium and calcium have been found to have open-shell singlet while the third-order complexes, Mg-$(C_4H_4$-Mg$)_3$ and Ca-$(C_4H_4$-Ca$)_3$ have triplet ground states. The spin flip from singlet diradical to triplet diradical is favored energetically with increasing size of complexes. The second hyperpolarizability of **MIS-I** and **MIS-II** complexes of Mg and Ca having intermediate diradical character has been predicted reasonably larger than that of the corresponding high spin triplets. In the triplet spin state the second hyperpolarizability increases gradually with increase of the size of metal complexes (**MIS-I** < **MIS-II** < **MIS-III**). The UBHHLYP, UCAM-B3LYP, UMP2 AND UCASSCF methods predict the correct qualitative trend of second hyperpolarizability of open-shell singlet MIS complexes of Mg and Ca.

Acknowledgements

(PKN) acknowledges the grant from UGC, Government of India under the Major Research Project (F. No. 42-339/2013 (SR) for carrying out this research work.

References

[1] P.N. Prasad, D.J. Williams, Introduction to Nonlinear Optical Effects in Molecules and Polymers, Wiley-Interscience, New York, 1991.
[2] F. Mayers, S. Marder, J.W. Perry, Introduction to the Nonlinear Optical Properties of Organic Materials in Chemistry of Advanced Materials, Wiley-VCH, New York, 1998.
[3] M.G. Papdopoulos, A.J. Sadlej, J. Leszczysnki, Non-Linear Optical Properties of Matter, Challenges and Advances in Computational Chemistry and Physics, Springer, 2006.
[4] G. Maroulis, Atoms, Molecules and Clusters in Electric Field, Imperial College Press, World Scientific, 2006.
[5] D.R. Kanis, M.A. Ratner, T.J. Marks, Chem. Rev. 94 (1994) 195.
[6] S.D. Bella, Chem. Soc. Rev. 30 (2001) 355.
[7] S.G. Raptis, M.G. Papadopoulos, A.J. Sadlej, Phys. Chem. Chem. Phys. 2 (2000) 3393.
[8] S. Eisler, A.D. Slepkov, E. Elliot, T. Luu, et al., J. Am. Chem. Soc. 127 (2005) 2666.
[9] B. Champagne, E.A. Perpete, D. Jacquemin, et al., J. Phys. Chem. A 104 (2000) 4755.
[10] J.W. Song, M.A. Watson, H. Sekino, K. Hirao, J. Chem. Phys. 129 (2008) 024117.
[11] P. Limacher, K.V. Mikkelsen, H.P. Luthi, J. Chem. Phys. 130 (2009) 194114.
[12] D. Lu, B. Marten, M. Ringnalda, R.A. Friesner, et al., Chem. Phys. Lett. 257 (1996) 224.
[13] Z.J. Li, F.F. Wang, Z.R. Li, H.L. Xu, et al., Phys. Chem. Chem. Phys. 11 (2009) 402.
[14] S. Bonness, H. Fukui, K. Yoneda, et al., Chem. Phys. Lett. 493 (2010) 195.
[15] M. Nakano, T. Kubo, et al., Chem. Phys. Lett. 418 (2006) 142.
[16] M. Nakano, H. Nagai, et al., Chem. Phys. Lett. 120 (2008) 467.
[17] W. Hu, H. Ma, C. Liu, Y. Jiang, J. Chem. Phys. 126 (2007) 044903.
[18] P. Karamanis, C. Pouchen, J. Phys. Chem. C 117 (2013) 3134.

[19] S.W. Tang, J.D. Feng, Y.Q. Qiu, H. Sun, et al., J. Comput. Chem. 32 (2011) 658.
[20] S.W. Tang, J.D. Feng, Y.Q. Qiu, H. Sun, et al., J. Comput. Chem. 31 (2010) 2650.
[21] E.N. Koukaras, A.D. Zdetsis, P. Karamanis, et al., J. Comput. Chem. 33 (2012) 1068.
[22] K. Hatua, P.K. Nandi, Comput. Theor. Chem. 996 (2012) 82.
[23] K. Hatua, P.K. Nandi, J. Theor. Comput. Chem. 12 (2013) 1350046.
[24] K. Hatua, P.K. Nandi, J. Theor. Comput. Chem. 12 (2013) 1350075.
[25] K. Hatua, P.K. Nandi, J. Phys. Chem. A 117 (2013) 16340.
[26] N. Liu, S. Gao, Y. Ding, Dalton Trans. 44 (2015) 345.
[27] A.D. Becke, J. Chem. Phys. 98 (1993) 5648.
[28] K. Yamaguchi, in: R. Carbo, M. Klobukowski (Eds.), Self-Consistent Field Theory and Applications, Elsevier, Amsterdam, 1990, p. 727.
[29] S. Yamanaka, M. Okumura, M. Nakano, K. Yamaguchi, J. Mol. Struct. 310 (1994) 205.
[30] A.D. Becke, J. Chem. Phys. 98 (1993) 1372.
[31] T. Yanai, D. Tew, N. Handy, Chem. Phys. Lett. 393 (2004) 51.
[32] H. Iikura, T. Tsuneda, T. Yanai, K. Hirao, J. Chem. Phys. 115 (2001) 3540.
[33] M.J. Frisch, G.W. Trucks, H.B. Schlegel, et al., Gaussian 09, Revision A.02, Gaussian, Inc., Wallingford, CT, 2009.
[34] T.J. Lee, P.R. Taylor, Int. J. Quantum Chem. Quant. Chem. Symp. S23 (1989) 199.
[35] R. Kishi, M. Nakano, S. Ohta, et al., J. Chem. Theory Comput. 3 (2007) 1699.